Hindawi Publishing Corporation
International Journal of Corrosion
Volume 2012, Article ID 927380, 9 pages
doi:10.1155/2012/927380

Research Article

Corrosion Behaviour of Heat-Treated Aluminum-Magnesium Alloy in Chloride and EXCO Environments

S. O. Adeosun, O. I. Sekunowo, S. A. Balogun, and V. D. Obiekea

Department of Metallurgical & Materials Engineering, University of Lagos, Nigeria

Correspondence should be addressed to S. O. Adeosun, samsonoluropo@yahoo.com

Received 12 September 2011; Revised 24 November 2011; Accepted 5 December 2011

Academic Editor: Rokuro Nishimura

Machines designed to operate in marine environment are generally vulnerable to failure by corrosion. It is therefore imperative that the corrosion susceptibility of such facilities is evaluated with a view to establishing mechanism for its mitigation. In this study, the corrosion behaviour of as-cast and retrogression-reagion (RRA) specimens of aluminum alloy containing 0.4–2.0 percent magnesium additions in NaCl, $FeCl_3$, and EXCO solutions was investigated. The corrosion simulation processes involved gravimetric and electrochemical techniques. Results show substantial inducement of Mg_2Si precipitates at a relatively higher magnesium addition, 1.2–2.0 percent, giving rise to increased attack. This phenomenon is predicated on the nature of the Mg_2Si crystals being anodic relative to the alloy matrix which easily dissolved under attack by chemical constituents. Formation of Mg_2Si intermetallic without corresponding appropriate oxides like SiO_2 and MgO, which protect the precipitates from galvanic coupling with the matrix, accentuates susceptibility to corrosion.

1. Introduction

Aluminum and its alloys are widely used in industry because of their light weight, high strength, and good corrosion resistance which is due to the formation of a protective oxide layer. However, under saline conditions such as those encountered in marine environments, aluminum alloys are vulnerable to localised degradation in forms of pitting and crevice corrosion. This type of corrosion involves the adsorption of an anion in particular chloride ion, Cl^-, at the oxide-solution interface.

In conventional metallic materials, the strong oxidizing power of the environment is required to establish spontaneous passivity; hence, to be of practical use, metallic materials must exhibit significant level of passivity in a given environment.

The passive stable surface film acts as a barrier for the transfer of cations from the metal to the environment and for the counter diffusion of oxygen and other anions. The air-formed film must be stable without damage to the underlying alloy surface in a given environment. Chemically homogenous, single-phase amorphous alloys free from crystalline defects such as precipitates, segregates, grain boundaries, and dislocations often create conducive environment for the formation of uniform passive film without any weak points [1].

Aluminum forms a protective oxide film in the pH range 4.0–8.5, but this depends on temperature, form of oxide present, and the presence of substances that form soluble complexes or insoluble salts with aluminum. This implies that the oxide film is soluble at pH values below 4.0 and above 8.5. However, Sziklarska and Smialowska [2] has reported the pitting potential of aluminum in chloride solutions to be relatively independent of pH in the range 4–9. This was further advanced by Godard [3] to demonstrate that a deviation from neutrality, PH 7, on both acid and alkaline sides increases the pitting rate in neutral fresh waters.

Corrosion behaviour of aluminum alloys is significantly affected by the presence of particles in the matrix [4]. Particles that contain Cu and Mg tend to be anodic relative to the alloy matrix, while those that contain Fe and Mn behave in cathodic manner relative to the matrix [5]. Previous works [6–8] show that Mg_2Si particles tend to be anodic in relation to the matrix and can act as initiation sites for corrosion. Most often the Mg_2Si phase dissolves leaving behind a cavity, which acts as a nucleation site for pitting

Table 1: Al-Mg alloy chemical composition.

No. of cast	% Composition										Si/Mg
	Fe	Si	Mn	Cu	Zn	Ti	Mg	Pb	Sn	Al	ratio
As-received	0.296	0.446	0.073	0.013	0.016	0.020	0.34	0.007	0.009	98.78	1.312
Alloy 1	0.269	0.584	0.024	0.096	0.021	0.013	0.42	0.009	0.004	98.56	1.390
Alloy 2	0.276	0.572	0.023	0.071	0.018	0.012	0.91	0.008	0.005	98.56	0.629
Alloy 3	0.219	0.403	0.021	0.002	0.003	0.014	1.23	0.001	0.007	98.10	0.328
Alloy 4	0.253	0.530	0.088	0.012	0.017	0.015	1.52	0.006	0.005	97.59	0.349
Alloy 5	0.414	0.599	0.025	0.019	0.015	0.013	1.81	0.005	0.004	97.10	0.331
Alloy 6	0.319	0.771	0.024	0.037	0.019	0.013	2.02	0.001	0.006	96.79	0.382

[9, 10]. These observations were made during investigations that were carried out on commercial aluminum alloys having low Si/Mg molar ratios [11–14].

Crevice corrosion is a highly localized form of corrosion which occurs by infiltration of water into closely fitted surfaces. The presence of aggressive ions such as chloride often creates extensive localized attack [4]. Chloride ions are drawn into the crevice as metal dissolution occurs and the conditions inside the crevice become acidic. Metals like aluminum that depend on oxide films or passive layers for corrosion resistance are particularly susceptible to crevice corrosion. Attack from this phenomenon can be aggravated when combined with the presence of crystalline defect such as Mg_2Si precipitates. Possibility exists for reducing drastically the alloy susceptibility to corrosion if its microstructure is modified by appropriate heat treatment prior to usage. In this study, the chemical response of heat-treated aluminium-magnesium alloy in chloride and acidic media was investigated.

2. Experimental Procedure

2.1. Materials. Ingots of 6063 aluminum alloy and magnesium used for this study were obtained from the Nigerian Aluminum Extrusion Company (NIGALEX). Six different compositions of Al-Mg alloy with chemical compositions shown in Table 1 were produced. The Mg in the alloy was varied between 0.40 and 2.0 percent.

The aluminum and magnesium alloy ingots were charged together into a crucible pot, heated to molten state, and then poured into a metal mould. Sufficient time was allowed for the cooling of cast samples prior to removal. Each cast sample was divided into sets A (a_i–a_l) and B (b_i–b_l) with set A samples left untreated while set B samples were retrogressed and aged (RRA). The samples in solution were heat treated at 475°C and aged for 24 hrs (T6 condition) after which the samples were retrogressed at 200°C, held for forty minutes, and quenched in water. The RRA samples were then tempered at 120°C for 24 hrs and allowed to cool in air.

Standard electrochemical corrosion coupons (Figure 1) and microstructural test specimens were prepared from both sets A and B samples. For electrochemical and gravimetric tests, Ø10 mm × 60 mm cylindrical rods and circular samples with dimensions of Ø14 mm ×4 mm were used, respectively.

Figure 1: Standard electrochemical corrosion specimen.

2.2. Corrosion Campaigns. The corrosion simulations were carried out on the RRA specimens using electrochemical polarization and gravimetric techniques in three different media, namely, salt, ferric chloride, and acid. Immersion test simulates corrosion resistance of alloy in chloride environment containing 10% salt in water saturated with oxygen at room temperature. The ferric chloride test is used to study the responses of Al-Mg alloy to crevice corrosion in a medium consisting of 5.6 mL of $FeCl_3 \cdot 6H_2O$, 2 g of NaCl, and 5 g of concentrated HCl in 300 mL of water. EXCO test studies exfoliation corrosion of Al-Mg alloy in severe industrial or marine environments containing 5 g of NaCl, 5 g of KNO_3, and 9 mL of HNO_3 in 300 mL of water. The Jenway 350-pH device was used to determine the pH of NaCl, $FeCl_3$, and EXCO solutions and the values are 6.80, 6.20, and 6.03, respectively.

In the gravimetric corrosion test, the initial weights of the test specimens were recorded before immersion in the test media while change in weights was taken every week using a Mettler Toledo weighing scale after the test pieces were rinsed in water and air-dried. The electrochemical corrosion set-up (Figure 2(a)) is similar to electrolytic process in which the aluminum-magnesium alloy coupon and copper act as anode and cathode electrodes, respectively. The electrodes were partially immersed in the media in separate containers as the anode coupon was connected to the positive terminal of a 12 V SMF 5219 battery while the copper electrode was connected to its negative terminal and a YEM 2210 variable resistor (Rheostat) was incorporated into the circuit. The drop in current flowing through the system was recorded at 20-minute interval using YEM 2011 ammeter (Figure 2(b)).

(a) (b)

Figure 2: Electrochemical setup. Electrical measuring devices

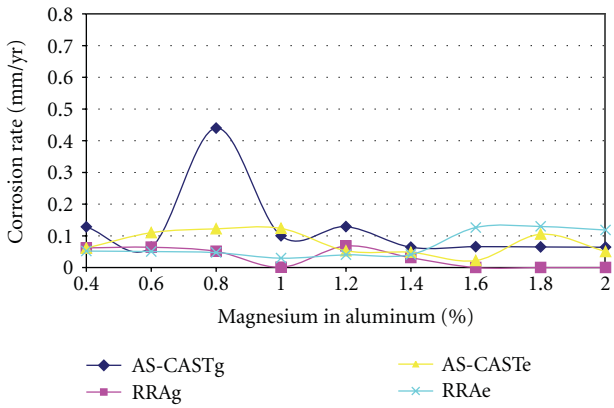

Figure 3: Effect of magnesium addition on the corrosion resistance of aluminum alloy in NaCl solution. Note**:** RRAg and AS-CASTg curves indicate the corrosion responses of heat-treated as-cast Al-Mg alloy specimens, respectively, in saline medium as evaluated through the gravimetric technique while RRAe and AS-CASTe curves illustrate the corrosion behaviors of heat-treated and as-cast Al-Mg alloy specimens, respectively, in saline environment as evaluated through the electrochemical polarization technique.

This electrochemical corrosion process lasted for six hours for each test piece studied.

2.3. Microstructure Analysis. Test specimens were prepared from the alloy samples and ground using emery grades of 40, 32, 10, and 8 in succession. The ground surfaces were polished using alumina paste to obtain a mirror-like surface. The polished test pieces were etched using dilute hydrochloric acid for 10s. The etched surfaces were carefully washed and dried. A digital Metallurgical Microscope at magnification of ×100 was used to obtain the morphology of the sample matrix, while the photomicrographs produced from these test specimens are shown in Figures 6–11.

3. Results and Discussion

3.1. Corrosion Rate Measurements. The corrosion susceptibility of test specimens in the various media (NaCl, $FeCl_3$, and EXCO solution) simulated was evaluated through both the gravimetric and electrochemical polarization techniques. This was carried out for the purposes of comparing which method can quickly provide information on the extent of corrosion on one hand and reliability of the data obtained on the other. Gravimetric corrosion measurement technique basically bothered on weight-loss regime of test specimens. In applying this method, the weights of test specimens were obtained before and at the end of time specified for each monitoring phase. Before the next phase of monitoring, the test specimens were thoroughly washed with water, air-dried, and weighed. The weight-loss data (Appendix A.1) obtained was used to compute the corrosion rate making use of the following relation:

$$\text{corrosion rate (mm/yr)} = \frac{87.6W}{\rho A t}, \tag{1}$$

where W is weight-loss (mg), ρ density of test specimen (gcm^{-3}), A area of test specimen (cm^2), and t exposure time (hr).

Electrochemical corrosion evaluation technique makes use of the electrical resistance property of test alloy by measuring the electrical polarization when current is impressed. In this study, standard test coupons of Al-Mg alloy of varying compositions were used as anode while copper was used as cathode. The set-up was partially immersed in each medium separately, and the drop in current flowing in through the system was recorded at 20-minutes interval. The corrosion rates as evaluated through (2) were presented in Appendix A.2.

$$\text{corrosion rate (mm/yr)} = \frac{3272WI_{\text{corr}}}{\rho A}, \tag{2}$$

where W is weight loss (g), ρ density of test specimen (gcm^{-3}), A *exposure surface* area of test specimen (cm^2), and I_{corr} current flowing in the test specimen (anode coupon).

The analyses of corrosion behaviour of test specimens by both gravimetric and electrochemical polarization show that the as-cast samples exhibited higher corrosion susceptibility than RRA specimens after immersion in NaCl solution (Figure 3). This trend subsists up to about 1.7% Mg addition in the aluminum alloy. The peak corrosion response of AS-CASTg: 0.13 mm/yr occurred at 0.4% and 1.2% Mg by gravimetric method while the electrochemical polarization technique recorded RRAe: 0.12 mm/yr at 0.91% and 1.81% Mg, respectively. In contrast to this observation, the RRA sample did not experience any appreciable corrosion within the period monitored (42 days) as computed using gravimetric technique. Through electrochemical polarization,

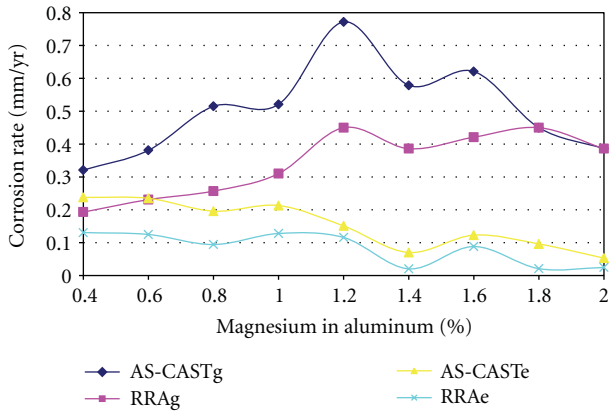

Figure 4: Effect of magnesium addition on the corrosion resistance of aluminum alloy in $FeCl_3$ solution. Note: RRAg and AS-CASTg curves indicate the corrosion responses of heat-treated and as-cast Al-Mg alloy specimens, respectively, in ferric chloride solution as evaluated through the gravimetric technique while RRAe and AS-CASTe curves illustrate the corrosion behaviors of heat-treated and as-cast Al-Mg alloy specimens, respectively, in ferric chloride solution as evaluated through the electrochemical polarization technique.

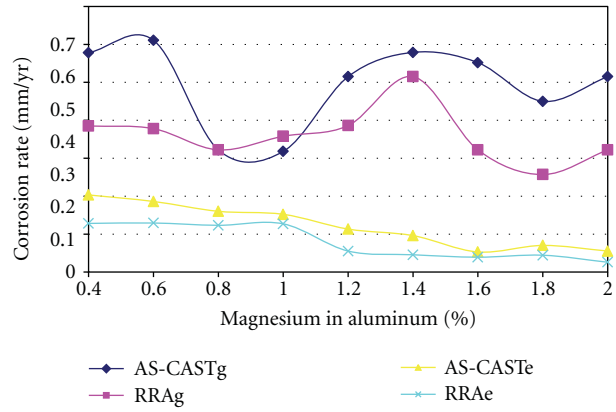

Figure 5: Effect of magnesium addition on the corrosion resistance of aluminum alloy in EXCO solution. Note: RRAg and AS-CASTg curves indicate the corrosion responses of heat-treated and as-cast Al-Mg alloy specimens, respectively, in EXCO solution as evaluated through the gravimetric technique while RRAe and AS-CASTe curves illustrate the corrosion behaviors of heat-treated and as-cast Al-Mg alloy specimens, respectively, in EXCO solution as evaluated through the electrochemical polarization technique.

however, the RRA test coupons exhibited some level of corrosion at 0.13 mm/yr for 1.5–2.02% Mg. The corrosion responses of the RRA test specimens in saline environment which contrast those of as-cast specimens can be attributed to the extensive microstructure evolution that occurred during heat treatment. The grains are relieved, refined, and homogenized. However, at higher magnesium addition, 1.2–2.02%, the corresponding high volume of Mg_2Si precipitated adversely impacted the alloys corrosion resistance.

The curves in Figure 4 illustrate the corrosion behavior of test specimens in ferric chloride environment. With regard to gravimetric corrosion measurement, the as-cast specimens show increasing corrosion propensity, AS-CASTg: 0.321–0.772 mm/yr for 0.42–1.23% Mg addition. Afterwards, the corrosion rate (AS-CASTg) dropped to 0.579 mm/yr for 1.51% Mg while some level of passivity was displayed at 1.81% Mg having just 0.45 mm/yr corrosion rate.

The rather sporadic corrosion pattern of the as-cast specimens is due largely to their microstructure inhomogeneity. This is confirmed by the RRAg: 0.45 mm/yr maximum corrosion rate by the RRA specimens because their microstructures have been refined by heat treatment.

The corrosion responses of as-cast and RRA samples in ferric chloride solution using electrochemical polarization technique measurement are also presented in Figure 4. Both the as-cast and RRA test coupons demonstrated similar corrosion rate pattern. Corrosion was more prevalent, AS-CASTe: 0.151–0.238 mm/yr and RRAe: 0.094–0.131 mm/yr for as-cast and RRA specimens, respectively, at a relatively low magnesium addition, 0.42–1.23%. However, at a relatively higher magnesium addition, 1.51–2.02%, corrosion rates dropped significantly to 0.053–0.056 mm/yr for as-cast and 0.020–0.025 mm/yr for RRA test coupons. Given this scenario, the electrochemical polarization corrosion measurement has proved that there is a strong correlation between the alloy structural integrity and corrosion susceptibility.

Figure 5 depicts the responses of test coupons to exfoliation corrosion under severe industrial and marine conditions (EXCO). Using the electrochemical polarization technique, the corrosion behaviors of both the as-cast and RRA samples are relatively low and nonuniform, AS-CASTe: 0.055–0.113 mm/yr and RRAe: 0.023–6–0.055 mm/yr for the as-cast and RRA specimens, respectively.

The inhomogeneity of microstructure must have been responsible for the wide range in corrosion rates exhibited by the as-cast specimens. Evaluation of the corrosion rates on the as-cast specimens through gravimetric method also shows that corrosion is nonuniform and the values are relatively high, AS-CASTg: 0.579 mm/yr and 0.322 mm/yr being the minimum. The RRA specimens, however, exhibited relatively uniform corrosion rates, RRAg: 0.257–0.386 mm/yr for the various magnesium additions. This is due to structural modifications that occurred pursuant to the heat treatment carried out on the alloy.

The microstructure of the as-cast specimens (Figure 6(a_i)) shows phases that are not evenly dispersed in the α-aluminum matrix, while there is strong clustering of Mg_2Si in certain area of the matrix. This is a potential polarization site for electrochemical attack on the alloy. The RRA specimens however have their Mg_2Si crystals fairly distributed within the matrix (Figure 6(b_i)).

Dipping of these specimens in NaCl solution gave rise to a substantial depletion of crystals of Mg_2Si and other intermetallics. This observation was more pronounced in the as-cast specimens (Figures 6(a_j), 6(b_j)) while the RRA alloy exhibited higher resistance to corrosion in NaCl solution than in $FeCl_3$ (Figures 6(b_j), 6(b_k)). In EXCO solution, the clustering arrangement of Mg_2Si crystals was preserved in

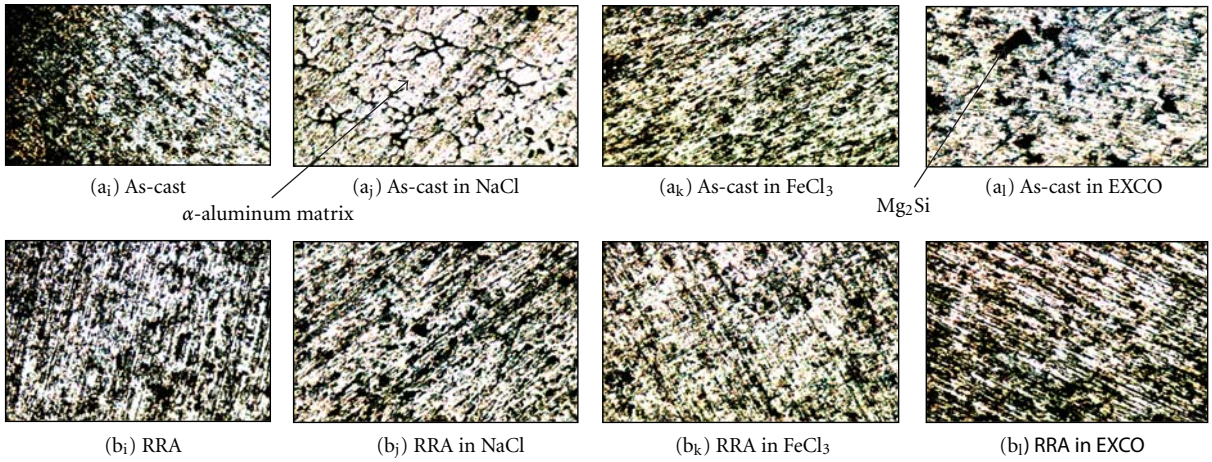

Figure 6: Micrographs of 0.42% Mg addition for untreated (a_i–a_l) and treated (b_i–b_l) specimens.

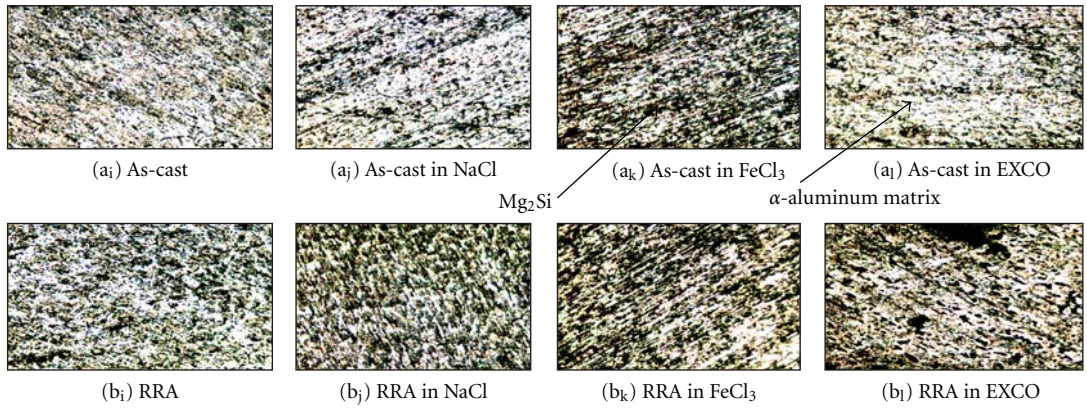

Figure 7: Micrographs of 0.91% Mg addition for untreated (a_i–a_l) and treated (b_i–b_l) specimens.

both alloy specimens (Figures 6(a_l), 6(b_l)) but the depletion of other intermetallics in the as-cast specimens was more than those of RRA alloy specimens. At 0.9% Mg addition, both alloy specimens have a fairly high volume fraction of Mg_2Si precipitates present in the matrices (Figures 7(a_i), 7(b_i)). On immersion in NaCl solution, the as-cast matrix is strongly attacked with significant erosion of the intermetallic phases while the RRA specimens show superior resistance to attack (Figures 7(a_k), 7(b_j).

Both the precipitates and intermetallic phases, however, remain stable in $FeCl_3$ solution (Figures 7(a_k), 7(b_k)) while erosion of magnesium silicides was observed with the as-cast alloy in EXCO solution (Figures 7(a_l), 7(b_l)). Fine crystals of magnesium silicides made appearance at 1.2% Mg addition (Figures 8(a_i), 8(b_i)).

The crystals remain stable in the matrices of both alloys when dipped in NaCl solution (Figures 8(a_j), 8(b_j)). In $FeCl_3$ solution, however, severe erosion of the intermetallic crystals which is more pronounced in as-cast matrix was observed (Figures 8(a_k), 8(b_k)) while the response of both specimens was not quite apparent in EXCO solution (Figures 8(a_l), 8b_l)). In Figure 9, the aluminum alloy specimens that contain 1.5% Mg have fine crystals induced in their structure (Figures 9(a_i), 9(b_i)). The intermetallic phase in the RRA alloy matrix was severely eroded in NaCl solution leaving the Mg_2Si crystals intact (Figures 9(a_j), 9(b_j)). However in $FeCl_3$, the corrosion behaviour of as-cast specimens is similar to that of RRA specimens, and Mg_2Si phase shows more resistance than other intermetallics (Figures 9(a_k), 9(b_k)). In Figures 9(a_l), 9(b_l) the as-cast alloy was strongly attacked in EXCO solution while substantial volume of Mg_2Si crystals induced in RRA specimens was retained.

In Figures 10(a_i), 10(b_i), higher volume fraction of intermetallics was observed in as-cast structure while clustering of Mg_2Si crystals occurred in RRA specimens. When immersed in NaCl solution, the as-cast matrix significantly corroded leaving only a few traces of the intermetallic crystals. The RRA suffered serious attack of its crystals than as-cast specimens in $FeCl_3$ solution with Mg_2Si crystals been washed off along with other intermetallics.

In EXCO solution, considerable corrosion occurred in the as-cast specimens thereby leaving the matrix almost bare (Figure 10(a_l)). The RRA alloy matrix, however, exhibited resistance to corrosion in EXCO solution, but, significant

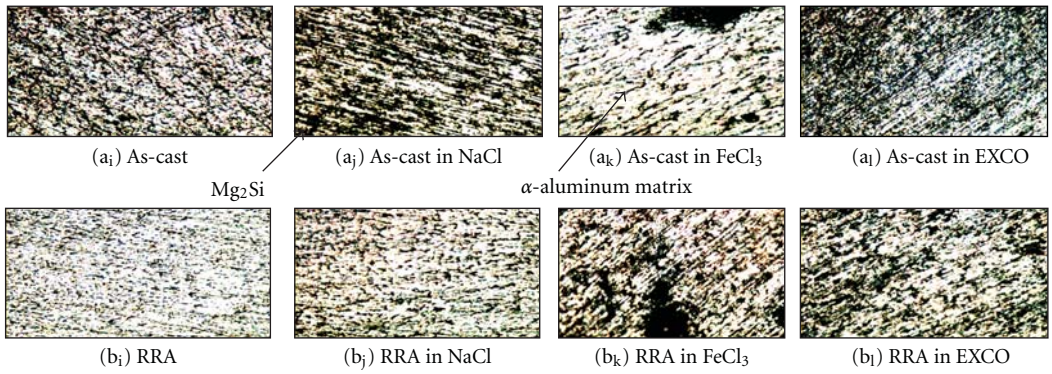

Figure 8: Micrographs of 1.23% Mg addition for untreated (a_i–a_l) and treated (b_i–b_l) specimens.

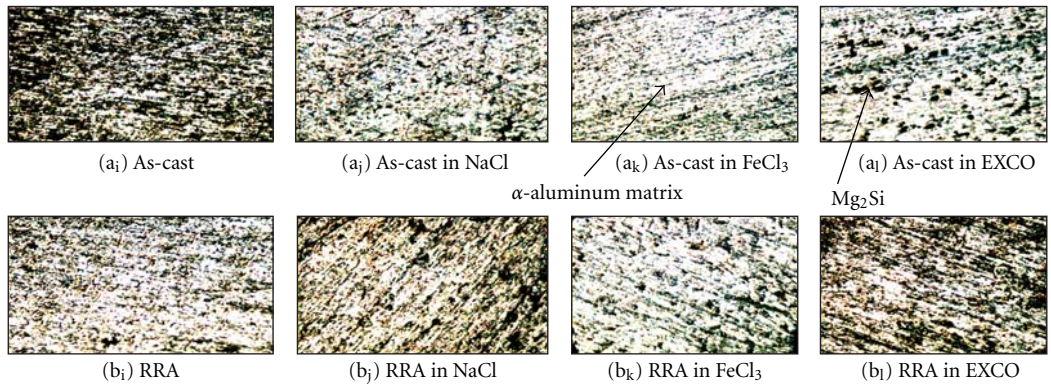

Figure 9: Micrographs of 1.51% Mg addition for untreated (a_i–a_l) and treated (b_i–b_l) specimens.

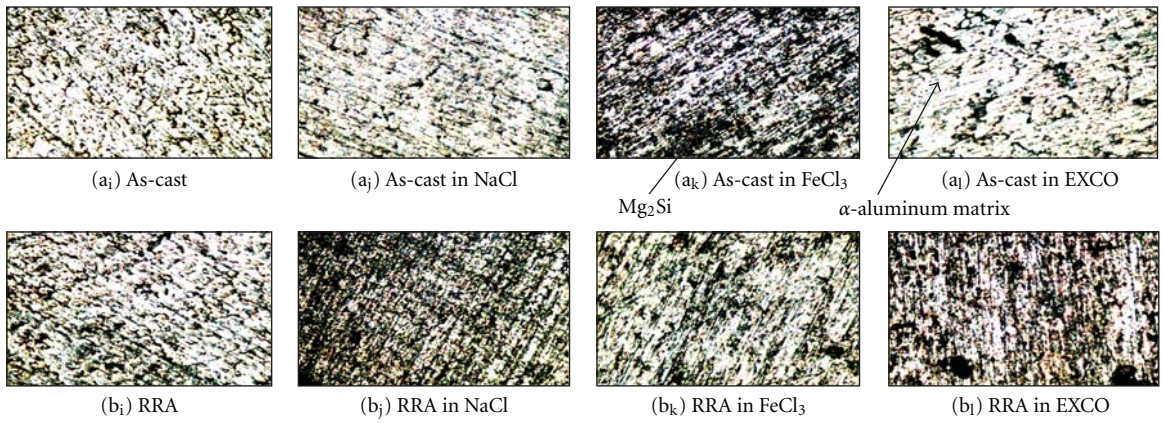

Figure 10: Micrographs of 1.81% Mg addition for untreated (a_i–a_l) and treated (b_i–b_l) specimens.

amount of Mg_2Si crystals was eroded leaving pit-like features in the matrix. (Figure 10(b_l)).

Figure 11 shows low volume fractions of Mg_2Si crystals in the RRA specimens at 2.0% Mg addition (Figure 11(b_i)). Strong erosion of the Mg_2Si crystals occurred in the as-cast matrix when dipped in NaCl solution but the other intermetallics were resistant in this medium (Figures 11(a_j), 11(b_j)). In $FeCl_3$ solution, the intermetallics show resistance to attack in both as-cast and RRA matrices but suffered the loss of crystals of $\acute{\alpha}$-aluminum to corrosion (Figures 11(a_k), 11(b_k)). Immersion of the alloy specimens in EXCO solution resulted in severe attack on the crystals of RRA matrix while the intermetallics in as-cast show superior resistance to the crystals of $\acute{\alpha}$-aluminum in this medium (Figures 11(a_l), 11(b_l)).

4. Conclusion

Corrosion responses of the as-cast and RRA alloy specimens differ significantly based on the microstructure induced in

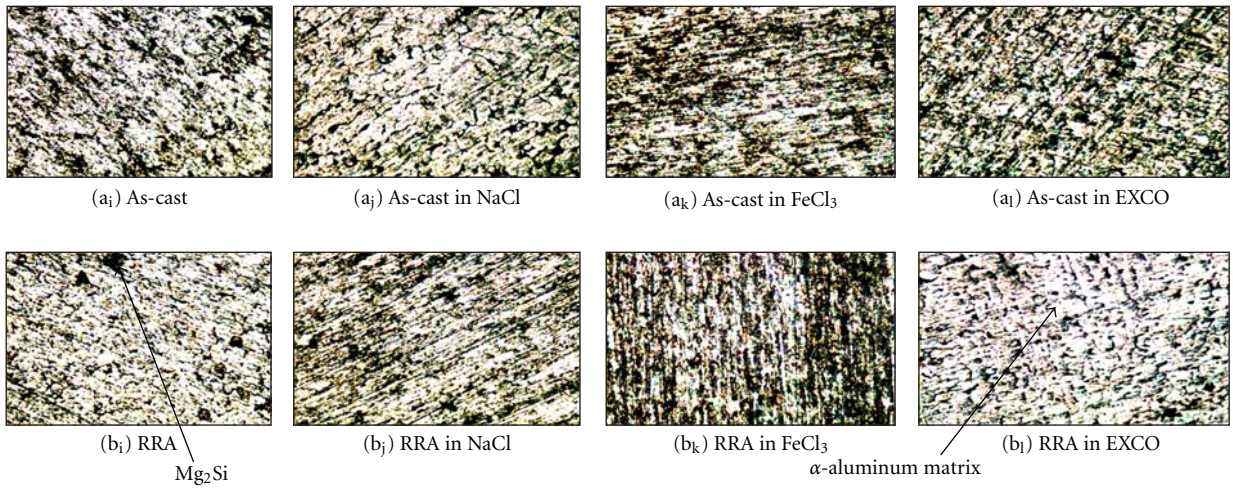

Figure 11: Micrographs of 2.02% Mg addition for untreated (a_i–a_l) and treated (b_i–b_l) specimens.

Table 2: Gravimetric corrosion rate (mm/yr) for the 0.42% Mg specimen.

Days	NaCl solution		$FeCl_3$		EXCO solution	
	As-cast	RRA	As-cast	RRA	As-cast	RRA
0	0	0	0	0	0	0
7	0	0	0.385	0	0.381	0.385
14	0	0	0.385	0.193	0.578	0.193
21	0	0	0.385	0.128	0.514	0.257
28	0.096	0	0.289	0.193	0.578	0.385
35	0.077	0	0.308	0.231	0.617	0.385
42	0.128	0.064	0.321	0.193	0.578	0.385

Table 3: Gravimetric corrosion rate (mm/yr) for the 0.91% Mg specimen.

Days	NaCl solution		$FeCl_3$		EXCO solution	
	As-cast	RRA	As-cast	RRA	As-cast	RRA
0	0.000	0.000	0.000	0.000	0.000	0.000
1200	0.000	0.000	0.771	0.000	0.000	0.000
2400	0.000	0.000	0.771	0.193	0.193	0.193
3600	0.000	0.000	0.642	0.257	0.128	0.257
4800	0.000	0.000	0.578	0.289	0.193	0.385
6000	0.077	0.000	0.54	0.231	0.231	0.308
7200	0.064	0.000	0.515	0.257	0.322	0.322

Table 4: Gravimetric corrosion rate (mm/yr) for the 1.23% Mg specimen.

Days	NaCl solution		$FeCl_3$		EXCO Solution	
	As-cast	RRA	As-cast	RRA	As-cast	RRA
0	0.000	0.000	0.000	0.000	0.000	0.000
7	0.000	0.000	1.542	0.771	0.000	0.385
14	0.000	0.000	1.156	0.771	0.385	0.385
21	0.128	0.000	1.028	0.514	0.514	0.514
28	0.096	0.000	0.963	0.482	0.482	0.482
35	0.154	0.000	0.848	0.463	0.540	0.463
42	0.129	0.064	0.772	0.450	0.515	0.386

Table 5: Gravimetric corrosion rate (mm/yr) for the 1.51% Mg specimen.

Days	NaCl solution		$FeCl_3$		EXCO solution	
	As-cast	RRA	As-cast	RRA	As-cast	RRA
0	0.000	0.000	0.000	0.000	0.000	0.000
7	0.000	0.000	1.156	1.156	0.771	0.000
14	0.000	0.000	0.964	0.578	0.578	0.385
21	0.000	0.000	0.899	0.385	0.642	0.514
28	0.000	0.000	0.771	0.385	0.578	0.482
35	0.077	0.000	0.694	0.385	0.54	0.463
42	0.064	0.000	0.579	0.386	0.579	0.515

them. The precipitated Mg_2Si crystals are anodic relative to the alloy matrix which easily dissolved under attack by chemical. This phenomenon occurred at relatively higher magnesium content in the range of 1.2–2.0%. Within this range, the volume fraction of Mg_2Si precipitates in the alloy matrix is rather substantial thereby accentuating susceptibility to corrosion.

Heat treatment process employed in this study serves the purpose of modifying the alloy microstructure such that inducement of soluble precipitates is suppressed in preference to strongly refractory intermetallics. This behavior was observed in the RRA specimens compared with as-cast alloy specimens thereby validating established significant role of the presence of intermetallics in an alloy matrix with respect to corrosion mitigation [15]. Intermetallics are complex compounds which do not easily dissolve thereby becoming cathodic relative to the alloy matrix. Therefore, the extent of corrosion suffered by an alloy depends on which phase

Table 6: Gravimetric corrosion rate (mm/yr) For the 1.81% Mg specimen.

Days	NaCl solution		$FeCl_3$		EXCO solution	
	As-cast	RRA	As-cast	RRA	As-cast	RRA
0	0.000	0.000	0.000	0.000	0.000	0.000
7	0.000	0.000	0.771	0.771	0.771	0.385
14	0.000	0.000	0.771	0.771	0.771	0.385
21	0.000	0.000	0.642	0.514	0.514	0.385
28	0.000	0.000	0.578	0.578	0.482	0.289
35	0.000	0.000	0.54	0.54	0.463	0.231
42	0.000	0.000	0.45	0.45	0.45	0.257

Table 7: Gravimetric corrosion rate (mm/yr) for the 2.02% Mg specimen.

Days	NaCl solution		$FeCl_3$		EXCO Solution	
	As-cast	RRA	As-cast	RRA	As-cast	RRA
0	0.000	0.000	0.000	0.000	0.000	0.000
7	0.000	0.000	0.771	0.771	0.385	0.000
14	0.000	0.000	0.385	0.771	0.578	0.193
21	0.000	0.000	0.514	0.514	0.514	0.578
28	0.000	0.000	0.482	0.482	0.482	0.514
35	0.077	0.000	0.463	0.385	0.54	0.308
42	0.064	0.064	0.386	0.386	0.515	0.322

Table 8: Gravimetric corrosion rate (mm/yr) for the control specimen.

Days	NaCl solution		$FeCl_3$		EXCO solution	
	As-cast	RRA	As-cast	RRA	As-cast	RRA
0	0	0	0	0	0	0
7	0	0	0.771	0.771	0.771	0.384
14	0	0	0.771	0.771	0.771	0.385
21	0.129	0	0.642	0.514	0.642	0.385
28	0.096	0	0.578	0.482	0.674	0.289
35	0.154	0.077	0.54	0.385	0.694	0.308
42	0.193	0.192	0.45	0.386	0.643	0.322

Table 9: Electrochemical corrosion rate For the 0.42% Mg specimen.

T (sec)	NaCl solution		$FeCl_3$		EXCO solution	
	As-cast	RRA	As-cast	RRA	As-cast	RRA
0	0.0000	0.0000	0.0000	0.0000	0.0000	0.0000
1200	0.0117	0.0123	0.0425	0.0394	0.0370	0.0238
2400	0.0224	0.0238	0.0850	0.0468	0.0727	0.0460
3600	0.0324	0.0338	0.1254	0.0690	0.1072	0.0666
4800	0.0425	0.0443	0.1643	0.0904	0.1429	0.0871
6000	0.0511	0.0544	0.1982	0.1109	0.1725	0.1089
7200	0.0614	0.0520	0.2378	0.1307	0.2033	0.1282

Table 10: Electrochemical corrosion rate for the 0.91% Mg specimen.

T (sec)	NaCl solution		$FeCl_3$		EXCO solution	
	As-cast	RRA	As-cast	RRA	As-cast	RRA
0	0.0000	0.0000	0.0000	0.0000	0.0000	0.0000
1200	0.0242	0.0061	0.0363	0.0176	0.0308	0.0238
2400	0.0468	0.0117	0.0702	0.0345	0.0605	0.04600
3600	0.0678	0.0167	0.1035	0.0499	0.0877	0.0653
4800	0.0871	0.0214	0.1355	0.0653	0.1129	0.0855
6000	0.1027	0.0252	0.1663	0.0785	0.1360	0.01048
7200	0.1233	0.0296	0.1959	0.0943	0.1601	0.1232

Table 11: Electrochemical corrosion rate for the 1.23% Mg specimen.

T (sec)	NaCl solution		$FeCl_3$		EXCO solution	
	As-cast	RRA	As-cast	RRA	As-cast	RRA
0	0	0	0	0	0	0
1200	0.0115	0.0057	0.0298	0.0234	0.0234	0.0119
2400	0.021	0.0105	0.0565	0.0435	0.0435	0.0222
3600	0.0302	0.0148	0.0816	0.0628	0.0616	0.0308
4800	0.0386	0.0185	0.1068	0.0805	0.0805	0.0394
6000	0.0750	0.0216	0.1283	0.0985	0.0965	0.0482
7200	0.0530	0.0401	0.1509	0.1158	0.1133	0.0554

Table 12: Electrochemical corrosion rate for the 1.51% Mg specimen.

T (sec)	NaCl solution		$FeCl_3$		EXCO solution	
	As-cast	RRA	As-cast	RRA	As-cast	RRA
0	0	0	0	0	0	0
1200	0.0056	0.0287	0.0169	0.0055	0.0226	0.0115
2400	0.0103	0.0524	0.0308	0.0099	0.0411	0.021
3600	0.0142	0.0739	0.0425	0.0136	0.0579	0.0283
4800	0.0173	0.0924	0.053	0.0165	0.0707	0.0337
6000	0.0195	0.1103	0.0616	0.018	0.0842	0.04
7200	0.0222	0.1263	0.0702	0.0203	0.0961	0.0456

Table 13: Electrochemical corrosion rate for the 1.81% Mg specimen.

T (sec)	NaCl solution		$FeCl_3$		EXCO solution	
	As-cast	RRA	As-cast	RRA	As-cast	RRA
0	0	0	0	0	0	0
1200	0.0172	0.0282	0.023	0.0056	0.0172	0.0113
2400	0.032	0.0524	0.0411	0.0101	0.0308	0.0201
3600	0.0434	0.0739	0.0579	0.0136	0.0425	0.0277
4800	0.0517	0.0944	0.0723	0.0165	0.053	0.0345
6000	0.0585	0.1129	0.0842	0.0185	0.0631	0.04
7200	0.105	0.1294	0.0961	0.0209	0.0702	0.0444

Table 14: Electrochemical corrosion rate for the 2.02% Mg specimen.

T (sec)	NaCl solution		$FeCl_3$		EXCO solution	
	As-cast	RRA	As-cast	RRA	As-cast	RRA
0	0	0	0	0	0	0
1200	0.0117	0.0242	0.0119	0.0058	0.0117	0.0058
2400	0.0222	0.046	0.0226	0.0107	0.0222	0.0107
3600	0.034	0.0653	0.0314	0.0151	0.032	0.0148
4800	0.0386	0.0838	0.0402	0.0189	0.0419	0.0189
6000	0.0452	0.1027	0.0472	0.0216	0.0493	0.0226
7200	0.0505	0.1183	0.053	0.0246	0.0554	0.0259

Table 15: Electrochemical corrosion rate for the control specimen.

T (sec)	NaCl solution		$FeCl_3$		EXCO solution	
	As-cast	RRA	As-cast	RRA	As-cast	RRA
0	0	0	0	0	0	0
1200	0.0119	0.0242	0.0119	0.0111	0.0176	0.0113
2400	0.0226	0.0468	0.023	0.021	0.0333	0.0214
3600	0.0326	0.069	0.0326	0.0302	0.049	0.0308
4800	0.0419	0.0904	0.0427	0.0386	0.0628	0.0402
6000	0.0513	0.1109	0.0523	0.047	0.0785	0.0493
7200	0.0604	0.1331	0.0616	0.0554	0.0924	0.0567

predominates, either soluble or indissoluble precipitates. The electrochemical corrosion evaluation provided a complimentary result when compared to the gravimetric method. However, the latter often takes months before any visible corrosion attack could be detected while the former takes just few minutes. This can be a crucial factor for determining the best approach to adopt in corrosion assessment where time is a constraint.

Appendices

A. Gravimetric and Electrochemical Corrosion Rates Data for Test Specimens in Various Environments

A.1. Gravimetric Corrosion Rates Data for Test Specimens in Various Media (Exposure Time: 42 Days). For more details, please see Tables 2, 3, 4, 5, 6, 7, and 8.

A.2. Electrochemical Corrosion Rates Data for Test Specimens in Various Media (Exposure Time: 2 Hours). For more details, please see Tables 9, 10, 11, 12, 13, 14, and 15.

References

[1] K. Hashimoto, "2002 W.R. Whitney award lecture: in pursuit of new corrosion-resistant alloys," *Corrosion*, vol. 58, no. 9, pp. 715–722, 2002.

[2] Z. Sziklarska-Smialowska, *Pitting Corrosion of Metals*, National Association of Corrosion Engineers, Houston, Tex, USA, 1986.

[3] H. G. Godard, *The Corrosion of Light Metals*, John Wiley & Sons, New York, NY, USA, 1967.

[4] L. Garrigues, N. Pebere, and F. Dabosi, "An investigation of the corrosion inhibition of pure aluminum in neutral and acidic chloride solutions," *Electrochimica Acta*, vol. 41, no. 7-8, pp. 1209–1215, 1996.

[5] R. P. Wei, C. M. Liao, and M. Gao, "A transmission electron microscopy study of constituent-particle-induced corrosion in 7075-T6 and 2024-T3 aluminum alloys," *Metallurgical and Materials Transactions A*, vol. 29, no. 4, pp. 1153–1160, 1998.

[6] K. A. Yasakau, M. L. Zheludkevich, S. V. Lamaka, and M. G. S. Ferreira, "Role of intermetallic phases in localized corrosion of AA5083," *Electrochimica Acta*, vol. 52, no. 27, pp. 7651–7659, 2007.

[7] J. H. W. De Wit, "Local potential measurements with the SKPFM on aluminium alloys," *Electrochimica Acta*, vol. 49, no. 17-18, pp. 2841–2850, 2004.

[8] F. Andreatta, H. Terryn, and J. H. W. de Wit, "Effect of solution heat treatment on galvanic coupling between intermetallics and matrix in AA7075-T6," *Corrosion Science*, vol. 45, no. 8, pp. 1733–1746, 2003.

[9] N. Birbilis and R. G. Buchheit, "Electrochemical characteristics of intermetallic phases in aluminum alloys : an experimental survey and discussion," *Journal of the Electrochemical Society*, vol. 152, no. 4, pp. B140–B151, 2005.

[10] J. Wloka, G. Bürklin, and S. Virtanen, "Influence of second phase particles on initial electrochemical properties of AA7010-T76," *Electrochimica Acta*, vol. 53, no. 4, pp. 2055–2059, 2007.

[11] A. Pardo, M. C. Merino, S. Merino, M. D. López, F. Viejo, and M. Carboneras, "Influence of SiCp content and matrix composition on corrosion resistance in cast aluminium matrix composites in salt fog," *Corrosion Engineering Science and Technology*, vol. 39, no. 1, pp. 82–88, 2004.

[12] S. Ren, X. He, X. Qu, I. S. Humail, and Y. Li, "Effect of Si addition to Al-8Mg alloy on the microstructure and thermophysical properties of SiCp/Al composites prepared by pressureless infiltration," *Materials Science and Engineering B*, vol. 138, no. 3, pp. 263–270, 2007.

[13] A. Pardo, M. C. Merino, R. Arrabal, S. Merino, F. Viejo, and A. E. Coy, "Effect of la surface treatments on corrosion resistance of A3xx.x/SiC p composites in salt fog," *Applied Surface Science*, vol. 252, no. 8, pp. 2794–2805, 2006.

[14] P. P. Trzaskoma and E. McCafferty, "Corrosion behavior of SiC/Al metal matrix composites," *Journal of the Electrochemical Society*, vol. 130, no. 9, pp. 1804–1809, 1983.

[15] J. Datta, C. Bhattacharya, and S. Bandyopadhyay, "Influence of Cl-, Br-, NO_3 and SO_2 Ions on the Corrosion Behaviour of 6061 Aluminium Alloy," *Indian Academy of Sciences, Bulletin of Materials Science*, vol. 28, no. 3, pp. 253–258, 2005.